Clinical Trial/Experimental Study

Medicine®

OPEN

MicroRNA-related transcription factor regulatory networks in human colorectal cancer

Shuhong Hao, MD[a,b], Sibo Huo, MD[c], Zhenwu Du, PhD[a,d], Qiwei Yang, PhD[a], Ming Ren, PhD[d], Shui Liu, MD[e], Tongjun Liu, PhD[c,*], Guizhen Zhang, PhD[a,d,*]

Abstract

Objective Colorectal cancer (CRC) is an extremely common gastrointestinal malignancy. The present study aimed to identify microRNAs (miRNAs) and transcription factors (TFs) associated with tumor development.

Methods Three miRNA profile datasets were integrated and analyzed to elucidate the potential key candidate miRNAs in CRC. The starBase database was used to identify the potential targets of common differentially expressed miRNAs (DEMs). Transcriptional Regulatory Element Database and Transcriptional Regulatory Relationships Unraveled by Sentence-based Text databases were used to identify cancer-related TFs and the TF-regulated target genes. Functional and pathway enrichment analyses were performed using the Database for Annotation, Visualization and Integration Discovery (DAVID) database, and the miRNA–TF–gene networks were constructed by Cytoscape. Quantitative reverse transcription polymerase chain reaction (qRT-PCR) was used to detect the expression of genes and miRNAs.

Results In total, 14 DEMs were found in CRC. By bioinformatics analysis, 5 DEMs (miR-145, miR-497, miR-30a, miR-31, and miR-20a) and 8 TFs (ELK4 (ETS-family transcription factor), myeloblastosis proto-oncogene like (MYBL)1, MYBL2, CEBPA, PPARA, PPARD, PPARG, and endothelial PAS domain protein (EPAS1)) appeared to be associated with CRC and were therefore used to construct miRNA–TF–gene networks. From the networks, we found that miR-20a might play the most important role as an miRNA in the networks. By qRT-PCR, we demonstrated that miR-20a was significantly upregulated in CRC tissues. We also performed qRT-PCR to identify the expression of miR-20a-related TFs (PPARA, PPARD, PPARG, EPAS1). Three of them, PPARA, PPARG, and EPAS1, were downregulated in CRC tissues, with statistically significant differences, while the downregulation of PPARD in CRC tissues was not significantly different. Pathway enrichment analyses indicated that the phosphoinositide 3-kinase (PI3K)-Akt signaling pathway was the most significantly enriched pathway. Two main elements of the PI3K-Akt signaling pathway, phosphatase and tensin homolog deleted on chromosome 10 and B-cell lymphoma 2-associated agonist of cell death, were demonstrated to be downregulated in CRC.

Conclusion The present study identified hub miRNAs and miRNA-related TF regulatory networks in CRC, which might be potential targets for the diagnosis and treatment of CRC.

Abbreviations: BAD = B-cell lymphoma 2-associated agonist of cell death, BP = biological process, CC = cellular component, CEBPA = CCAAT/enhancer binding protein A, CRC = colorectal cancer, DAVID = Database for Annotation, Visualization and Integration Discovery, DEM = differentially expressed miRNA, GEO = Gene Expression Omnibus, GO = Gene Ontology, HIF = hypoxia-inducible factor, KEGG = Kyoto Encyclopedia of Genes and Genomes, logFC = log fold change, MF = molecular function, miRNA = microRNA, mRNA = messenger RNA, NCBI = National Center for Biotechnology Information, NFI = nuclear factor I, PANT = paired adjacent normal tissues, PI3K = phosphoinositide 3-kinase, PPAR = peroxisome proliferator-activated receptor, PTEN = phosphatase and tensin homolog deleted on chromosome 10, qRT-PCR = quantitative reverse transcription polymerase chain reaction, STAT = signal transducer and activator of transcription, TCGA = The Cancer Genome Atlas, TF = transcription factor, TRED = Transcriptional Regulatory Element Database, TRRUST = Transcriptional Regulatory Relationships Unraveled by Sentence-based Text, VEGF = vascular endothelial growth factor.

Keywords: bioinformatics, colorectal cancer, microRNA, transcription factor

Editor: Sayed S. Daoud.

This work was supported by the project supported by the National Natural Science Foundation of China (Grant no. 81702195), and the Project of Application Demonstration Center of Precision Medicine for Molecular Diagnosis in Jilin Province (2016–2018, NDRC).

The authors have no conflicts of interest to disclose.

[a] Department of Medical Research Center, [b] Department of Hematology and Oncology, [c] Department of General Surgery, [d] Department of Orthopedics, [e] Department of Hepatobiliary and Pancreatic Surgery, The Second Hospital of Jilin University, Changchun, Jilin, China.

[*] Correspondence: Guizhen Zhang, Jilin University Second Hospital, Changchun, Jilin, China (e-mail: zhangguizhenjlu@163.com), Tongjun Liu (e-mail: tongjunliu@163.com).

Medicine (2019) 98:15(e15158)

Received: 7 November 2018 / Received in final form: 12 February 2019 / Accepted: 15 March 2019

http://dx.doi.org/10.1097/MD.0000000000015158

1. Introduction

Colorectal cancer (CRC) is the third most common cancer and the third leading cause of cancer-related deaths in men and women worldwide.[1] In America alone, in 2016, an estimated 134,490 cases of CRC were diagnosed, and 49,190 patients died of the disease.[2] Despite considerable advancements in the diagnosis, treatment, and understanding of the molecular mechanisms of CRC, the recurrence and metastasis of CRC continue to be closely associated with poor prognosis.[3] Therefore, a deeper understanding of the molecular mechanisms in CRC progression, as well as the identification of new therapeutic strategies and diagnostic and prognostic biomarkers, is urgently warranted.

MicroRNAs (miRNAs) are small, regulatory, noncoding RNAs that are mostly involved in messenger RNA (mRNA) degradation and post-transcriptional repression.[4] MiRNAs were first discovered in 1993, after which nearly 2000 human miRNAs have been identified, which have been shown to play important roles in various biological processes, including cell proliferation, cell cycle, apoptosis, and differentiation.[5] In humans, mounting evidence has implicated miRNA dysregulation in multiple diseases, including cancers, with different functional, tumor-suppressing, or oncogenic consequences in different contexts.[6] A study by Sun et al[7] found that miR-195–5p is dramatically downregulated in human CRC tissues compared with normal colorectal tissues, and that miR-195–5p can serve as a prognostic marker to predict the outcome of CRC patients. Qu et al[8] suggested that miR-374b inhibits colon cancer cell proliferation and invasion through the downregulation of Liver receptor homolog-1 expression. These findings highlight the promising applications of miRNAs as a novel approach for the diagnosis and therapy of patients with CRC.

MiRNAs function mainly by binding to their complementary sequence on target mRNA to negatively regulate their target genes at the post-transcriptional level.[9] Some of the targets of miRNA are genes encoding transcription factors (TFs). As the terminal regulators of gene expression, a TF binds to the DNA helix at specific regulatory sequences to activate or inhibit transcription.[10] MiRNA can affect the development of tumors by regulating TF expression. For example, Wang et al[11] found that miR-122 repressed c-Myc transcription by targeting the transcriptional activator E2f1 and coactivator Tfdp2 in hepatocellular carcinoma. Bao et al[12] found that in lung cancer, miR-1269 promotes cell survival and proliferation by targeting TP53, which is a TF suppressing tumor growth through the regulation of dozens of target genes with diverse biological functions.[13] However, studies on the systematic analysis of miRNA-related TF regulatory networks in CRC have been limited.

Therefore, in the present study, we analyzed 3 miRNA microarray datasets from Gene Expression Omnibus (GEO) to obtain differentially expressed miRNAs (DEMs) between CRC tissues and adjacent normal colorectal tissues by GEO2R. Using the prediction software, we obtained target genes corresponding to the DEMs. In addition, we selected cancer-related TFs from the target genes to construct miRNA–TF–gene networks. The potential mechanism by which miRNA regulates the proliferation and invasion of CRC through TFs was revealed.

2. Materials and methods

2.1. CRC miRNA profiling dataset analysis

The CRC datasets of miRNA array profiling with accession numbers GSE41655, GSE35834, and GSE48267 were selected by consulting the Gene Expression Omnibus DataSets portal (GEO DataSets), publicly available on the National Center for Biotechnology Information (NCBI) website (www.ncbi.nlm.nih.gov/geo/), including data from 125 CRC tissues and 99 paired adjacent normal tissues (PANT) collected from 3 different regions (China, Italy, and the USA). The DEMs between CRC and PANT were screened using GEO2R (http://www.ncbi.nlm.nih.gov/geo/geo2r), which is an interactive web tool for identifying the differential expression of genes across experimental conditions in a GEO series. |Log fold change| (|logFC|) >1 and $P < .05$ for the comparison between tumor and PANT were considered statistically significant. The DEMs from the 3 cohort profile datasets were overlapped by Venny 2.1 software (http://bioinfogp.cnb.csic.es/tools/venny/index.html).[14] Before the 3 datasets were overlapped, the miRNAs contained in all the datasets were annotated according to the last nomenclature published by miRBase v22 (http://www.mirbase.org/) because of the different microarray platforms considered.[15] The pipeline of the whole process of this study is shown in Figure 1.

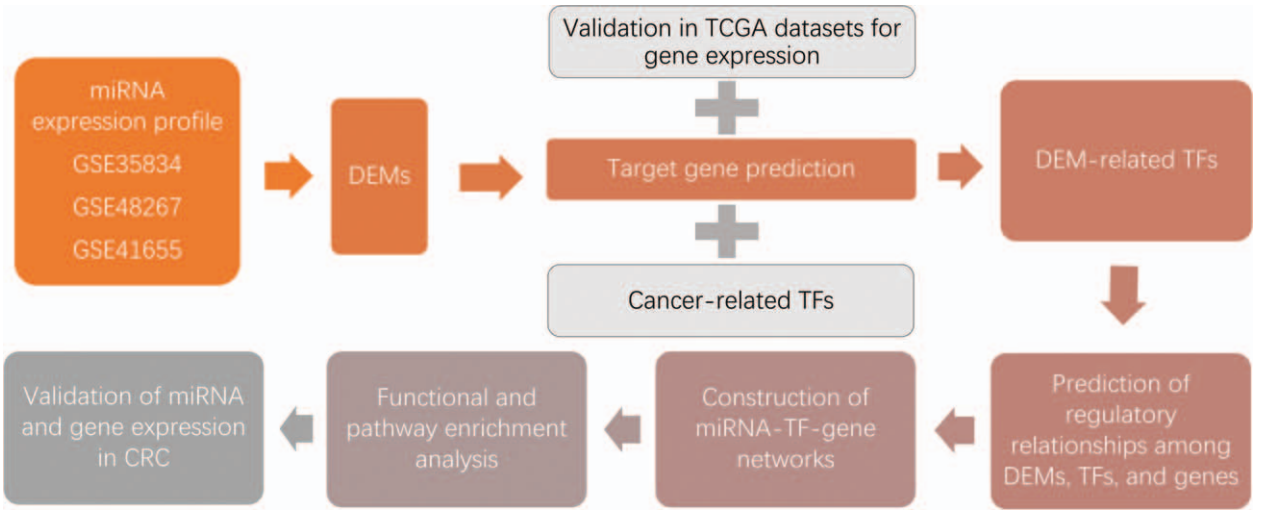

Figure 1. A schematic flow chart of the analysis steps. CRC = colorectal cancer, DEM = differentially expressed miRNA, miRNA = microRNA, TCGA = The Cancer Genome Atlas, TF = transcription factor.

2.2. Gene target analysis of selected miRNAs

The starBase v2.0 (http://starbase.sysu.edu.cn/) database is a bioinformatics prediction tool used to systematically identify the RNA–RNA and RNA–protein interaction networks from 108 CLIP-Seq (cross-linking, ligation, and sequencing of hybrids, Photoactivatable ribonucleoside-enhanced crosslinking and immunoprecipitation, individual-nucleotide resolution crosslinking and immunoprecipitation, high throughput sequencing-crosslinking and immunoprecipitation)-generated datasets.[16] In our study, the presumed targets of common DEMs were identified by starBase v2.0 with the selection criteria of high stringency; number of cancer types ≥2; and prediction in at least 2 databases among TargetScan, picTar, RNA22, PITA, and miRanda. By consulting the Transcriptional Regulatory Element Database (TRED) (http://rulai.cshl.edu/TRED), it was possible to identify 36 cancer-related TF families that are known to be involved in carcinoma development.[17] Subsequently, by overlapping the predicted target genes and 36 cancer-related TF families, DEM-targeted TFs that affect CRC proliferation were obtained.

2.3. Construction of miRNA–TF–gene networks

Transcriptional Regulatory Relationships Unraveled by Sentence-based Text mining database (TRRUST version 2.0) (www.grnpedia.org/trrust), a manually curated database of human transcriptional regulatory networks,[18] was used to obtain the target genes of TFs. For the validation of gene expression, UALCAN (http://ualcan.path.uab.edu), an interactive web portal for gene expression, and survival data analysis of The Cancer Genome Atlas (TCGA) database were used in this study, with $P < .05$ considered statistically significant.[19] Finally, miRNA–TF–gene networks were constructed based on miRNA expression profile, starBase, TRED, UALCAN, and TRRUST by Cytoscape 3.6.0 software (http://www.cytoscape.org/).

2.4. Functional and pathway enrichment analysis

Gene Ontology (GO) analysis is widely used to provide gene annotation terms for large-scale genomic or transcriptomic data,[20] and the Kyoto Encyclopedia of Genes and Genomes (KEGG) is used for pathway enrichment analysis.[21] In the present study, the functional and pathway enrichment of genes in the miRNA–TF–gene networks was analyzed using DAVID (version 6.8) (https://david.ncifcrf.gov/) by performing GO and KEGG analysis.[22] The results of GO analysis comprised 3 categories: biological process (BP), cellular component (CC), and molecular function (MF); $P < .05$ was selected as the threshold for significant GO terms and pathways.

2.5. Tissue samples

Twenty tissue samples, including 10 CRC and 10 PANT (distance from cancer >5 cm), were acquired by pathological assessment of tissues retrieved from surgeries, together with complete clinical information from patients at The Second Affiliated Hospital of Jilin University (Changchun, China) between February 2017 and December 2017. Samples were snap-frozen in liquid nitrogen immediately after tumor resection and stored at −80°C until further processing. No local or systemic neoadjuvant, radiotherapy, chemotherapy, or targeted therapy was provided. The study was approved by the Ethics Committee of The Second Affiliated Hospital of Jilin University. Informed consent forms were signed by all patients for the acquisition and use of tissue samples.

2.6. Total RNA extraction and quantitative polymerase chain reaction

Total RNA from clinical tissues was extracted with TRIzol reagent (Invitrogen, Carlsbad, CA) following the manufacturer's protocol. RNA concentration was measured using the NanoDrop 2000 spectrophotometer (Thermo Scientific, Waltham, MA). RNA (1 μg) was converted into cDNA with a First Strand cDNA Synthesis Kit (TransGen Biotech, Beijing, China), and quantitative polymerase chain reaction (qPCR) was performed with TransStart Top Green qPCR SuperMix (TransGen Biotech) on the Applied Biosystems 7500 Sequence Detection System (Thermo Scientific). For miRNA, quantitative reverse transcription PCR (qRT-PCR) was performed with the All-in-OneTM miRNA qRT-PCR Detection Kit (GeneCopoeia, Rockville, MD) on the Applied Biosystems 7500 Sequence Detection System. The relative expression levels of mRNAs and miRNAs were calculated using the $2^{-\Delta\Delta Ct}$ method[23] and were normalized to 18S and U6 RNA, respectively.

2.7. Statistical analysis

Statistical analysis of the results was performed using SPSS 22 software (SPSS, Inc., Chicago, IL). The comparisons of the mean values of the analyzed parameters were performed using Student *t* test. The obtained data (miRNA and mRNA levels) are presented as means ± standard deviation; $P < .05$ was considered to indicate a statistically significant difference.

3. Results

3.1. Identification of DEMs in CRC

CRC and PANT miRNA expression profiles of GSE41655, GSE35834, and GSE48267 were obtained from the NCBI-GEO database (Table 1). We extracted 63, 96, and 110 DEMs from the expression profile datasets GSE35834, GSE48267, and GSE41655, respectively, with thresholds of $|\log2FC| > 1.0$ and $P < .05$. On overlapping the DEMs from the 3 cohort profile data sets, we obtained 14 common DEMs (Table 2, Fig. 2A), including 8 upregulated miRNAs and 6 downregulated miRNAs in the CRC tissues, compared to PANT (Table 3). Employing Multi-

Table 1

The information of microRNA expression profiles.

Series	First author	Publication year	Country	Platform	Tumor site	Number of samples (normal/tumor)
GSE41655	Shi X	2015	China	GPL11487	CRC	48 (15/33)
GSE35834	Bortoluzzi S	2014	Italy	GPL8786	CRC	54 (23/31)
GSE48267	Li E	2015	USA	GPL10850	CC	122 (61/61)

CC = colon cancer, CRC = colorectal cancer.

Table 2

The number of differentially expressed microRNAs of expression profiles.

	Upregulation	Downregulation	Total
GSE41655	56	54	110
GSE35834	28	35	63
GSE48267	52	44	96
Commonly DEMs	8	6	14

DEMs = differentially expressed miRNAs.

Experiment Viewer (MeV version 4.7) (http://mev.tm4.org/), we developed a heatmap of the 8 upregulated and 6 downregulated DEMs of the 3 miRNA expression profiles, showing the significantly differential distribution of the 14 DEMs (Fig. 3).

3.2. Target gene prediction and cancer-related TF identification

To identify the potential target genes of the 14 DEMs, target prediction was performed using the bioinformatics tool starBase. A total of 1928 putative targets were identified (data not shown). By consulting TRED, we obtained 36 cancer-related TF families that are known to be involved in carcinoma development (Table 4). Subsequently, by overlapping the predicted target genes and TF families, we obtained 12 results (Fig. 2B), which were putative target genes of 8 miRNAs (Table 5). Because miRNAs mainly negatively regulate their target genes, the expression of target genes should run counter to the expression of their corresponding miRNAs. We further verified the expression of the 12 target genes in the TCGA colon adenocarcinoma database by UALCAN (including 41 normal colon tissues and 286 primary tumors). The results showed that the expression levels of ELK4, MYBL1, and MYBL2 were significantly higher in primary tumors than those in the normal colon for CRC patients from TCGA, in contrast to the expression levels of their corresponding miRNAs, miR-145, miR-497, and miR-30a, respectively ($P < .05$). The expression level of CEBPA was significantly lower in primary tumors than that in the normal colon for CRC patients from TCGA, in contrast to the expression level of its corresponding miRNA, miR-31 ($P < .05$). The expression levels of PPARA, PPARD, PPARG, and EPAS1 were significantly lower in primary tumors than that in the normal colon for CRC patients from TCGA, unlike the expression levels of their corresponding miRNA, miR-20a ($P < .05$) (Fig. 4). Except for the 8 genes, the expression levels of the other genes were consistent with their corresponding miRNAs or were not significantly different between primary tumor and normal colon tissue for CRC patients from TCGA ($P > .05$) (Table 5). Based on these results, we chose 5 miRNAs (miR-145, miR-497, miR-30a,

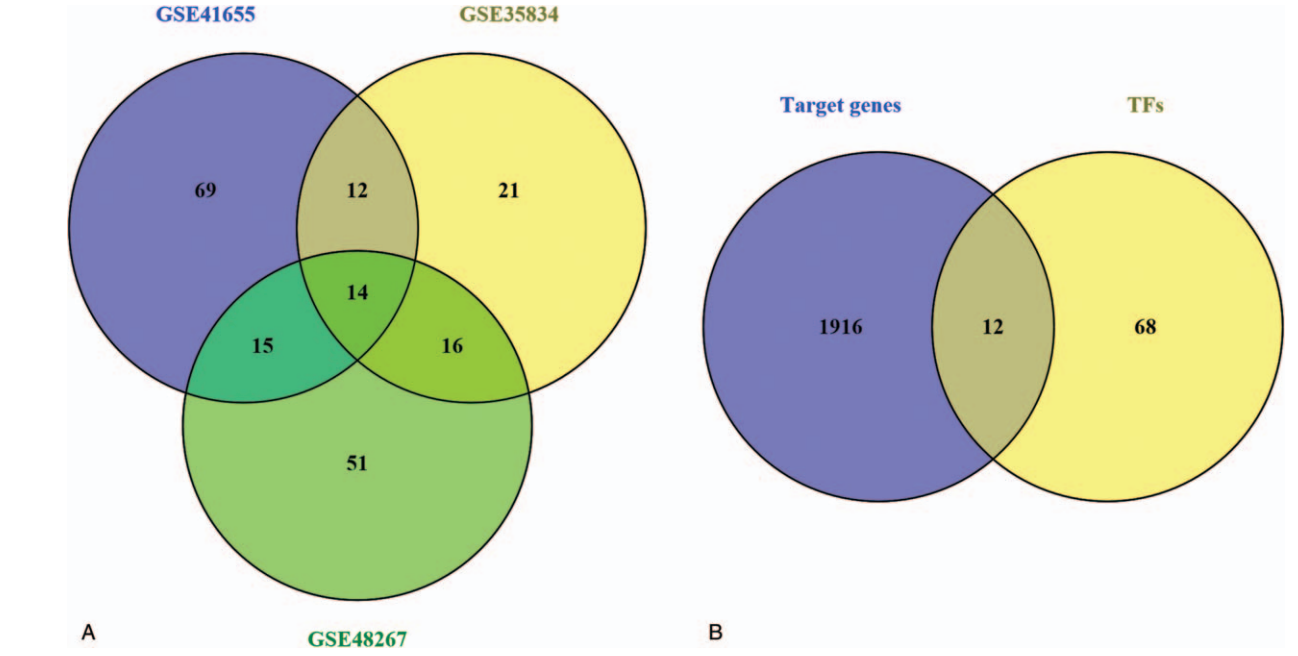

Figure 2. Venn diagrams. (A) Identification of common DEMs of the 3 cohort profile datasets. Different color areas represent different datasets. The overlapping areas are the common DEMs. (B) Identification of cancer-related TFs in the target genes of DEMs. The blue area represents the putative target genes of the common DEMs, and the yellow area represents 36 cancer-related TF families. DEM = differentially expressed miRNA, TF = transcription factor.

Table 3

The commonly differentially expressed microRNAs of 3 microRNA expression profiles.

Commonly DEMs	Gene symbol
Upregulated DEMs	hsa-miR-31, hsa-miR-224, hsa-miR-183, hsa-miR-18a, hsa-miR-20a, hsa-miR-1246, hsa-miR-552, hsa-miR-21
Downregulated DEMs	hsa-miR-378, hsa-miR-378*, hsa-miR-145, hsa-miR-497, hsa-miR-30a, hsa-miR-30a*

DEMs = differentially expressed miRNAs.

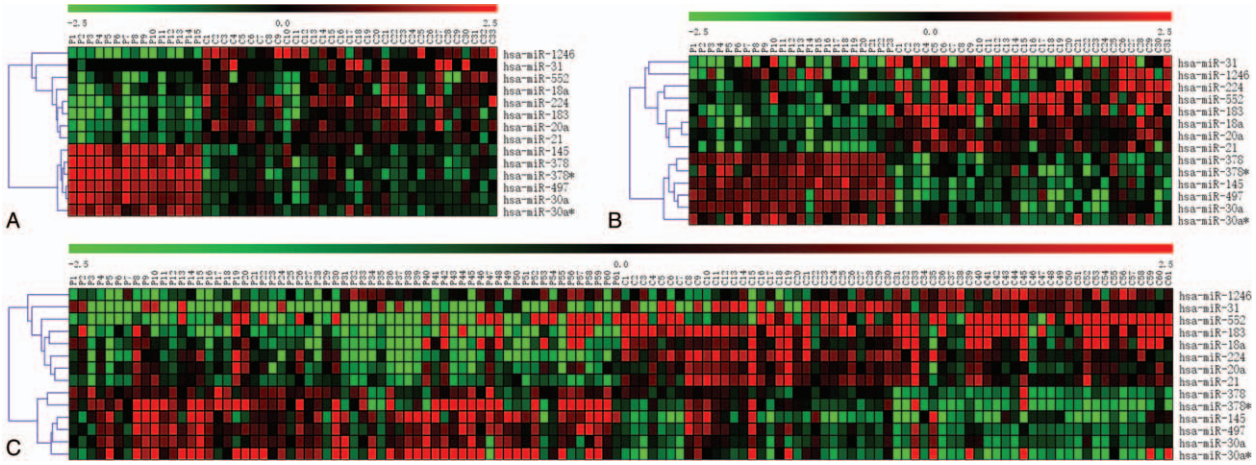

Figure 3. Clustering of the 14 DEMs in CRC vs. PANT across each independent dataset. (A) Clustering analysis of GSE41655. (B) Clustering analysis of GSE35834. (C) Clustering analysis of GSE48267. Each column represents a sample, and each row represents the expression level of a given miRNA. The color scale represents the raw score ranging from blue (low expression) to red (high expression). Dendrograms by each heatmap correspond to the hierarchical clustering by the expression of the 14 miRNAs. CRC = colorectal cancer, DEM = differentially expressed miRNA, miRNA = microRNA, PANT = paired adjacent normal tissues.

Table 4

Curated 36 cancer-related transcription factor families.

Family	Full name	Members (official gene symbols)
AP1	Activator protein 1	FOS, FOSB, JUN, JUNB, JUND
AP2	Activator protein 2	TFAP2A, TFAP2B, TFAP2C, TFAP2D, TFAP2E
AR	Androgen receptor	AR
ATF	Activating transcription factor	ATF1–7
BCL	B-cell CLL/lymphoma	BCL3, BCL6
BRCA	Breast cancer susceptibility protein	BRCA1–3
CEBP	CCAAT/enhancer binding protein	CEBPA, CEBPB, CEBPD, CEBPE, CEBPG
CREB	cAMP responsive element binding protein	CREB1–5, CREM
E2F	E2F transcription factor	E2F1–7
EGR	Early growth response protein	EGR1–4
ELK	Member of ETS oncogene family	ELK1, ELK3, ELK4
ER	Estrogen receptor	ESR1, ESR2
ERG	ETS -related gene	ERG
ETS	ETS-domain transcription factor	ETS1, ETS2, ETV4, SPI1
FLI1	Friend leukemia integration site 1	FLI1
GLI	Glioma-associated oncogene homolog	GLI1–4
HIF	Hypoxia-inducible factor	HIF1A, ARNT, EPAS1, HIF3A
HLF	Hepatic leukemia factor	HLF
HOX	Homeobox gene	HOXA, HOXB, HOXD series, CHX10, MSX1, MSX2, TLX1, PBX2
LEF	Lymphoid enhancing factor	LEF1
MYB	Myeloblastosis oncogene	MYB, MYBL1, MYBL2
MYC	Myelocytomatosis viral oncogene homolog	MYC
NFI	Nuclear factor I; CCAAT-binding transcription factor	NFIA, NFIB, NFIC, NFIX
NFKB	Nuclear factor kappa B, reticuloendotheliosis oncogene	NFKB1, NFKB2, RELA, RELB, REL
OCT	Octamer binding proteins	POU2F1–3, POU3F1–2, POU5F1
p53	P53 family	TP53, TP73L, TP73
PAX	Paired box gene	PAX1–9
PPAR	Peroxisome proliferator-activated receptor	PPARA, PPARD, PPARG
PR	Progesterone receptor	PGR
RAR	Retinoic acid receptor	RARA, RARB, RARG
SMAD	Mothers against decapentaplegic homolog	SMAD1–9
SP	Sequence-specific transcription factor	SP1–8
STAT	Signal transducer and activator of transcription	STAT1–6
TAL1	T-cell acute lymphocytic leukemia-1 protein	TAL1
USF	Upstream stimulatory factor	USF1, USF2
WT1	Wilms tumor 1 (zinc finger protein)	WT1

cAMP = adenosine-3',5'-cyclic monophosphate, CLL = chronic lymphocytic leukaemia, ELK = ETS-family transcription factor, EPAS = endothelial PAS domain protein, ETS = E Twenty Six-specific, LRH = liver receptor homolog, MYBL = myeloblastosis proto-oncogene like.

Table 5

MicroRNAs containing transcription factors in target genes.

miRNA	Target genes/TFs	Expression (miRNA/target genes)
hsa-miR-145	ELK4	↓/↑
hsa-miR-497	MYBL1	↓/↑
hsa-miR-30a	MYBL2	↓/↑
hsa-miR-31	CEBPA	↑/↓
hsa-miR-20a	PPARA, PPARD, PPARG, EPAS1	↑/↓
	ELK3, ELK4	↑
	HIF1A, NFIB	–
hsa-miR-18a	HIF1A	↑/–
hsa-miR-21	NFIA,NFIB	↑/–
hsa-miR-224	NFIA,NFIB	↑/–

↑ = higher expressed in colorectal cancer, ↓ = lower expressed in colorectal cancer, – = no differential expression between colorectal cancer and normal colon, CEBPA = CCAAT/enhancer binding protein A, HIF = hypoxia-inducible factor, miRNA = microRNA, MYBL = myeloblastosis proto-oncogene like, NFI = nuclear factor I, PPAR = peroxisome proliferator-activated receptor, TF = transcription factor.

miR-31, and miR-20a) and 8 TFs (ELK4, MYBL1, MYBL2, CEBPA, PPARA, PPARD, PPARG, and EPAS1) to fulfill our next objective of constructing miRNA–TF–gene networks.

3.3. Construction of miRNA–TF–gene networks

By searching the target genes of the 8 TFs through the TRRUST version 2 database, we obtained 161 genes, which were downstream genes of the 8 TFs. We further verified the expression of these genes in TCGA by UALCAN. The results showed that 116 of the genes had differential expression between primary tumors and the normal colon for CRC patients from TCGA ($P > .05$) (Table 6). Based on these results, we constructed the miRNA–TF–gene networks with the 5 miRNAs, 8 TFs, and 116 target genes by Cytoscape 3.6.0 software (Fig. 5). From the networks, we found that miR-20a might be playing the most important miRNA role in the networks. MiR-20a interacted with 4 TFs (PPARA, PPARD, PPARG, and EPAS1) and indirectly interacted with 95 target genes in these networks. Second, miR-31, which indirectly interacted with 39 target genes through 1 transcription factor (CEBPA), also seemed to play an important role in this network.

3.4. Functional annotation and pathway enrichment analysis of the genes in the miRNA–TF–gene networks

We performed GO and KEGG pathway analysis for the 116 target genes in the miRNA–TF–gene networks using DAVID software. The annotation of the 116 target genes was mainly classified into 3 functional groups: BP, CC, and MF (Table 7, Fig. 6). As shown inFigure 6, in the BP group, the top 3 enriched terms were mainly cellular response to hypoxia, release of cytochrome c from mitochondria, and response to hydrogen peroxide. In terms of CC, the top 3 enriched terms were extracellular space, extracellular region, and extracellular matrix. In addition, MF analysis also revealed that the target genes were significantly enriched in growth factor activity, identical protein binding, and hormone activity. Moreover, KEGG pathway analysis indicated that the phosphoinositide 3-kinase (PI3K)-Akt, FoxO, and hypoxia-inducible factor-1 signaling pathways were the top 3 significantly enriched pathways (Table 8, Fig. 7).

3.5. Quantitative reverse transcription polymerase chain reaction

Twenty samples from 10 patients, including 6 men and 4 women, were used to perform qRT-PCR. The age at diagnosis ranged from 43 to 79 years. Primary tumors were observed in the colon of 3 patients and in the rectum of 7 patients. The histological subtypes pure adenocarcinoma and mucinous adenocarcinoma were found in 9 and 1 patients, respectively. The staging of

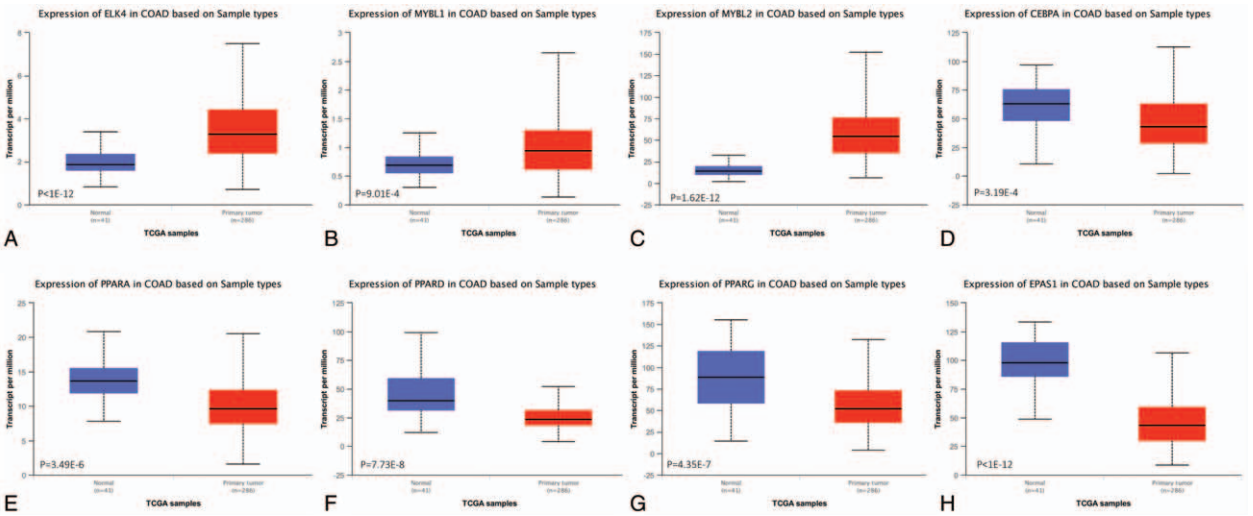

Figure 4. Identification of the expression levels of the target genes in the TCGA colon adenocarcinoma database. (A–C) The expression levels of ELK4, MYBL1, and MYBL2 were significantly higher in primary tumors than in the normal colon, in contrast to the expression levels of their corresponding miRNAs, miRNA 145, miRNA 497, and miRNA 30a, respectively ($P < .05$). (D) The expression level of CEBPA was significantly lower in primary tumors than that in the normal colon, which was in contrast to the expression level of its corresponding miRNA, miRNA 31 ($P < .05$). (E–H) The expression levels of PPARA, PPARD, PPARG, and EPAS1 were significantly lower in primary tumors than that in the normal colon for CRC patients from TCGA, which was in contrast to the expression levels of their corresponding miRNA, miRNA 20a ($P < .05$). CEBPA = CCAAT/enhancer binding protein A, CRC = colorectal cancer, miRNA = microRNA, PPAR = peroxisome proliferator-activated receptor, TCGA = The Cancer Genome Atlas.

Table 6

Differently expressed target genes of the transcription factors.

Transcription factor	Target genes
ELK4	NR2C2
MYBL1	DHRS2, NCL
MYBL2	CCNA1, CCND1, COL1A1, MYBL2, MYC, NCL,
CEBPA	AFP, ALB, BCL2, CD163, CSF1, CSF3R, DEFA1, DEFA3, ELANE, FN1, GAPDH, HAMP, HK3, HOMER3, HSD17B11, HSPA4, ICAM1, IGF1, IGF2, IL10, IL5, IL6, INSR, ITGAX, MAD1L1, MSR1, MYC, PCK1, PCK2, PRL, S100A9, SAA1, SLC10A1, SPI1, SPP1, STAR, STAT3, TLR9, VLDLR
PPARA	ACADL, ACOX1, ACSL1, APOB, APOBR, CD36, CETP, CGB5, CPT1A, FABP4, G0S2, HMOX1, IGFBP1, IL6, IL6R, LPL, MLYCD, MMP9, NFKBIA, PDK4, PLIN2, PTGS2, SERPINE1, SLC25A20, SLC9A1, SOD2, SREBF2, TUBA1B, TXNIP, UGT1A9
PPARD	ANG, CAT, HSD11B2, PDK4, SAT1, SOD1, TIMP1, TXN
PPARG	ABCG2, ACAT1, AGER, APOBR, BAD, BCL2, BCL2L1, CAT, CAV1, CCND1, CCNE1, CD36, CDKN1A, CEBPA, CLDN2, CPT1B,CSF1, DEFB103A, EGFR, ERO1A, FASLG, GDF15, HMOX1, ICAM1, KLF4, MMP1, MMP9, MYC, NOTCH4, NR1H3, PDK2, POU2F1, PTEN, PTGS2, REN, RETN, SAT1, SERPINE1, SLC2A4, SLC9A1, SOCS7, TG, TNFRSF11B, TP53, TSHR, TXNIP, UGT1A9, VLDLR
EPAS1	CA9, CCR7, COL10A1, FLT1, MMP14, MSC, PTPRZ1, SERPINE1, VEGFA

CEBPA = CCAAT/enhancer binding protein A, PPAR = peroxisome proliferator-activated receptor, MYBL = myeloblastosis proto-oncogene like.

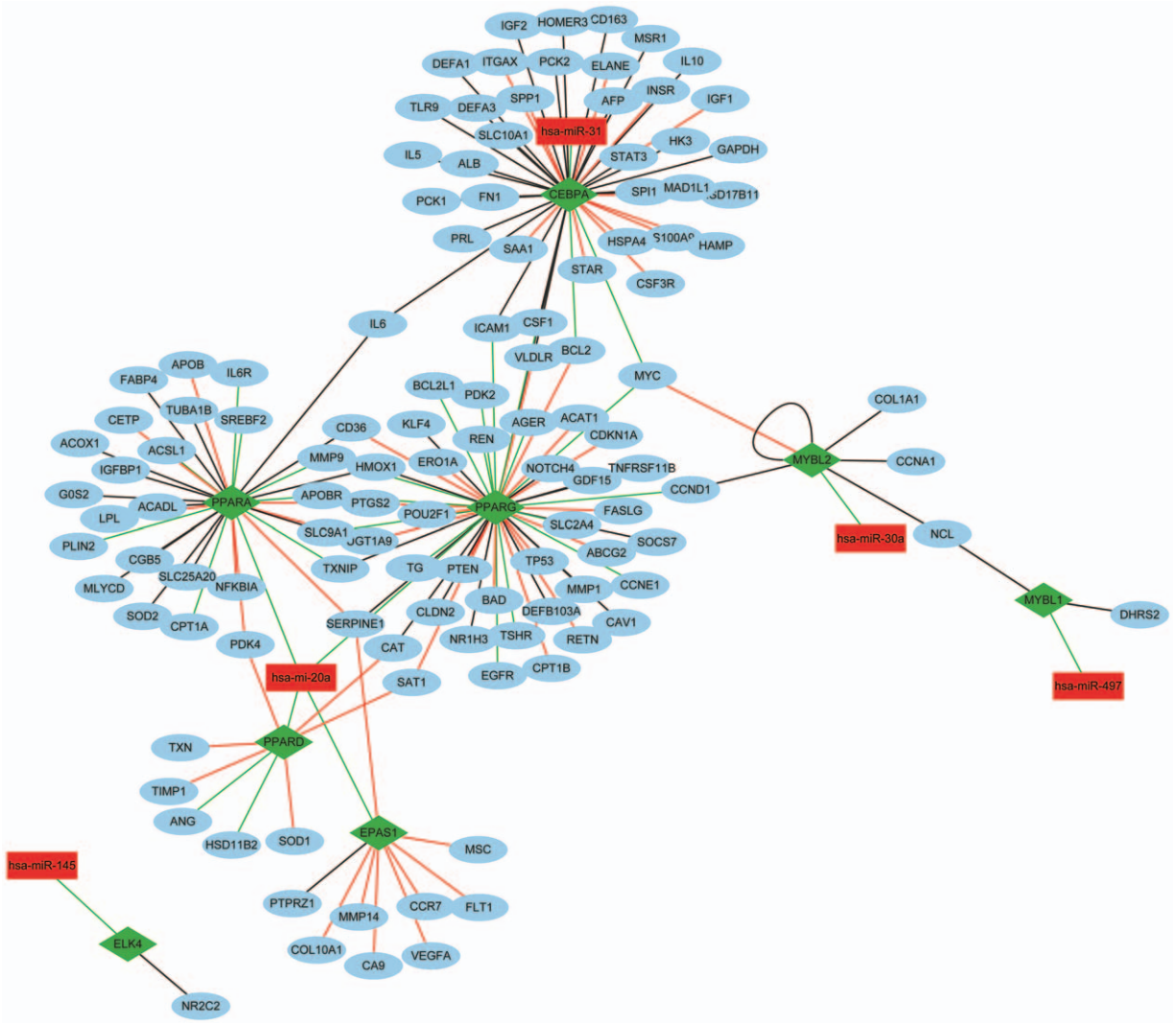

Figure 5. MiRNA–TF–gene regulatory networks for CRC. The red square nodes represent miRNAs; green diamond nodes, TFs; and blue ellipsoidal nodes, the target genes of TFs. The lines represent the interaction between 2 nodes, with red for activation, green for repression, and gray for unknown. CRC = colorectal cancer, miRNA = microRNA, TF = transcription factor.

Table 7

Gene annotation of the target genes of transcription factor.

1. Top 10 enriched biological process of target genes.

GO name	GO_ID	*P* value	Count
Cellular response to hypoxia	GO:0071456	2.35E-05	6
Release of cytochrome c from mitochondria	GO:0001836	8.08E-05	4
Response to hydrogen peroxide	GO:0042542	2.18E-04	4
Response to gamma radiation	GO:0010332	3.83E-04	4
Regulation of multicellular organism growth	GO:0040014	3.83E-04	4
Regulation of mitochondrial membrane Permeability	GO:0046902	3.85E-04	3
transcription, DNA-templated	GO:0006351	5.50E-04	10
Regulation of mitochondrial membrane potential	GO:0051881	6.14E-04	4
Negative regulation of apoptotic process	GO:0043066	.001035201	8
Intrinsic apoptotic signaling pathway in response to DNA damage	GO:0008630	.00103699	4

2. Top 10 enriched cellular component of target genes.

GO name	GO_ID	*P* value	Count
Extracellular space	GO:0005615	9.42E-09	24
Extracellular region	GO:0005576	.001073524	11
Extracellular matrix	GO:0031012	.004949095	5
Mitochondrion	GO:0005739	.006546907	13
Cytosol	GO:0005829	.008398587	13
Mitochondrial outer membrane	GO:0005741	.009379296	4
RNA polymerase II transcription factor complex	GO:0090575	.01002836	3
Myelin sheath	GO:0043209	.011593544	5
Extracellular exosome	GO:0070062	.016054033	21
Mitochondrial matrix	GO:0005759	.024773456	4

3. Top 10 enriched molecular function of target genes.

GO name	GO_ID	*P* value	Count
Growth factor activity	GO:0008083	6.60E-05	6
Identical protein binding	GO:0042802	3.03E-04	5
Hormone activity	GO:0005179	9.41E-04	5
Kinase activity	GO:0016301	.002197826	5
Cytokine activity	GO:0005125	.003444331	6
Protein heterodimerization activity	GO:0046982	.004499169	4
Ubiquitin protein ligase binding	GO:0031625	.016159652	4
Phosphoenolpyruvate carboxykinase activity	GO:0004611	.017124514	2
Phosphoenolpyruvate carboxykinase (GTP) activity	GO:0004613	.017124514	2
Palmitoyl-CoA oxidase activity	GO:0016401	.017124514	2

GO = gene ontology.

patients following the American Classification Joint Committee on Cancer showed 2 patients classified as stage I, 3 patients as stage II, and 5 patients as stage III.

From the miRNA–TF–gene networks, we found that miR-20a might be playing the most important miRNA role for CRC. Therefore, we performed qRT-PCR to examine the expression of miR-20a and TFs that interacted with miR-20a, including PPARA, PPARD, PPARG, and EPAS1 in CRC. The relative expression of miR-20a was 1.84 ± 0.73 folds upregulated in tumor tissues versus the adjacent nontumor tissues ($P < .01$). The relative expression levels of PPARA, PPARG, and EPAS1 were 0.36 ± 0.15 ($P < .01$), 0.26 ± 0.18 ($P < .01$), and 0.48 ± 0.28 ($P < .05$) folds downregulated in tumor tissues versus adjacent nontumor tissues, respectively. The relative expression of PPARD was 0.87 ± 0.57 folds downregulated in tumor tissues versus the adjacent nontumor tissues, but this was not statistically significant. Because the most enriched KEGG pathway of the target genes was the PI3K-Akt signaling pathway, we chose the main PI3K-Akt signaling pathway-related elements from the genes in the miRNA–TF–gene networks, including phosphatase and tensin homolog deleted on chromosome 10 (PTEN) and B-cell lymphoma 2-associated agonist of cell death (BAD), to perform qRT-PCR verification. The relative expression levels of PTEN and BAD were 0.50 ± 0.48 and 0.25 ± 0.36 folds downregulated in tumor tissues versus adjacent nontumor tissues, respectively (Fig. 8).

4. Discussion

CRC is a digestive tract tumor with a relatively high incidence rate among various malignant tumors.[1] In the past several decades, numerous studies have been conducted to understand the causes and underlying mechanisms of CRC occurrence and development; however, the incidence and mortality of CRC remain very high globally. This might be because studies often focus on a single genetic effect.[24] However, cancer genomics is complex, with underlying networks involving a variety of factors such as noncoding RNAs, coding genes, and TFs. The overall aim of the current study was to explore the correlation among miRNAs, TFs, and target genes in CRC.

Initially, we integrated 3 cohorts of profile datasets of individuals from 3 different geographical regions (China, Italy,

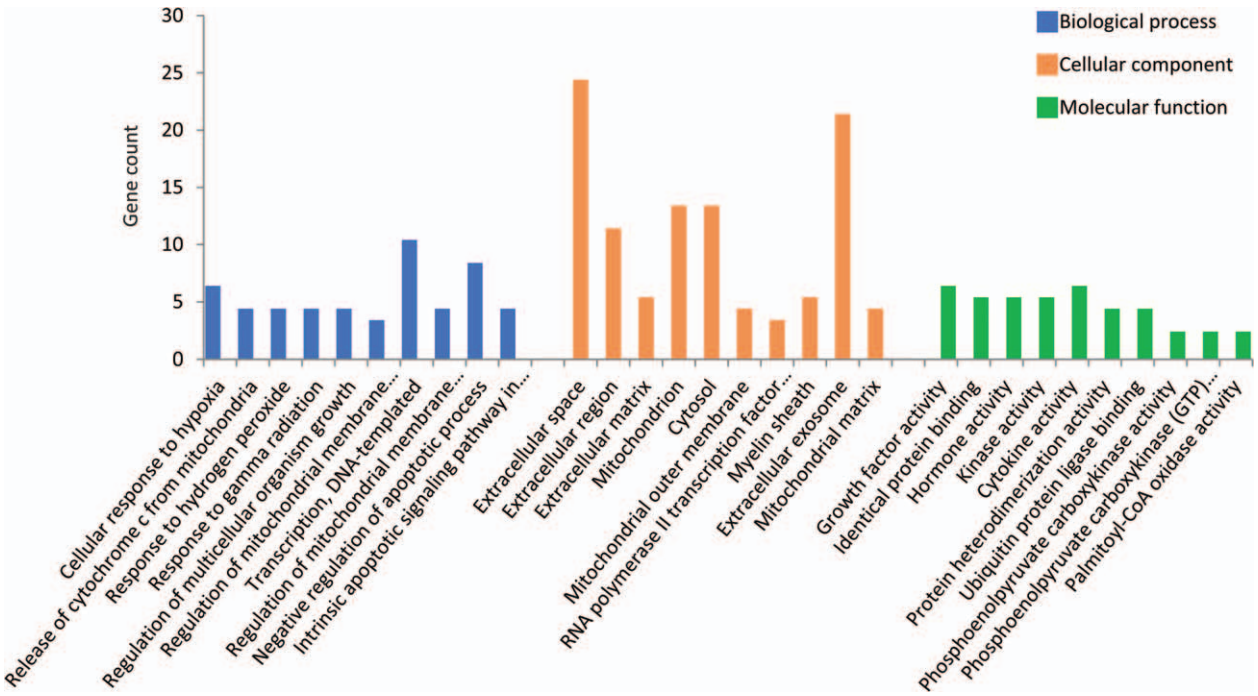

Figure 6. Gene Ontology of target genes in the miRNA–TF–gene networks. GO analysis classified the target genes into 3 groups (i.e., biological process, cellular component, and molecular function). GO = Gene Ontology, miRNA = microRNA, TF = transcription factor.

and the USA) and applied bioinformatics analysis to identify 14 commonly altered DEMs. By predicting the targets of the DEMs and the associated cancer-related TFs, we finally identified 5 miRNAs (miR-145, miR-497, miR-30a, miR-31, and miR-20a) that were considered to regulate CRC proliferation through TFs. By consulting the literature, we found that all the 5 miRNAs are related to the generation and proliferation of malignant tumors.[25–29] Among the 5 miRNAs, miR-20a was considered to be the most important miRNA in CRC because it interacted with 4 TFs (PPARA, PPARD, PPARG, and EPAS1), while the others interacted with only 1 TF. MiR-20a, a member of the miR-17–92 cluster, has been shown to function as an oncomir in CRC. A study performed by Cheng et al[30] demonstrated that miR-20a was upregulated in CRC and that it promoted CRC invasion and metastasis by downregulating Smad4. Xu et al[31] reported that miR-20a enhances the epithelial-to-mesenchymal transition of CRC cells by modulating matrix metalloproteinases. In the present study, on the basis of miRNA microarray data and qRT-PCR verification, we demonstrated that miR-20a was upregulated in CRC. The results were consistent with several studies. However, the result of qRT-PCR was not exactly the same as that of the microarray. In the qRT-PCR test, the relative expression of miR-20a was 1.84 ± 0.73 folds upregulated in CRC tissues compared to normal tissues, which was less than 2 folds. The strength of microarray-based techniques lies in their ability to quantify large numbers of miRNAs simultaneously in a single experiment. However, the specificity of microarray-based miRNA tests is lower than that of qRT-PCR tests.[32] Therefore, we believe that the results of qRT-PCR are more reliable. Of course, we cannot exclude the errors in the results of qRT-PCR tests, which could partly be due to the small sample number. Fan et al[33] reported that miR-20a overexpression suppresses the expression levels of PPARG in bone marrow stem cells, indicating that PPARG might be the direct target of miR-20a. The result of this study is consistent with the putative target of miR-20a in our study. Besides, in the present study, we found that the PI3K/Akt signaling pathway was the most significantly enriched pathway in the miRNA–TF–gene networks. This finding was similar to the report of Jiang et al,[34] which demonstrated that miR-20a

Table 8

Top 20 enriched Kyoto Encyclopedia of Genes and Genomes pathway of target genes.

Pathway name	Pathway ID	*P* value	Count
PI3K-Akt signaling pathway	ssc04151	4.48E-13	24
FoxO signaling pathway	ssc04068	1.24E-11	16
HIF-1 signaling pathway	ssc04066	6.10E-11	14
Pathways in cancer	ssc05200	1.19E-10	23
Hepatitis B	ssc05161	9.62E-09	14
Insulin resistance	ssc04931	3.73E-08	12
PPAR signaling pathway	ssc03320	4.54E-08	10
Proteoglycans in cancer	ssc05205	1.51E-07	14
Bladder cancer	ssc05219	1.65E-07	8
Prostate cancer	ssc05215	3.71E-07	10
Small cell lung cancer	ssc05222	4.11E-07	10
Transcriptional misregulation in cancer	ssc05202	9.78E-07	12
Adipocytokine signaling pathway	ssc04920	1.07E-06	9
Jak-STAT signaling pathway	ssc04630	3.18E-06	11
Cytokine–cytokine receptor interaction	ssc04060	5.51E-06	13
AMPK signaling pathway	ssc04152	5.58E-06	10
MicroRNAs in cancer	ssc05206	4.24E-05	12
Focal adhesion	ssc04510	5.35E-05	11
Pancreatic cancer	ssc05212	6.79E-05	7
Fatty acid degradation	ssc00071	7.63E-05	6

AMPK = Mitogen-activated protein kinase; HIF = hypoxia-inducible factor, PPAR = peroxisome proliferator-activated receptor, STAT = signal transducer and activator of transcription.

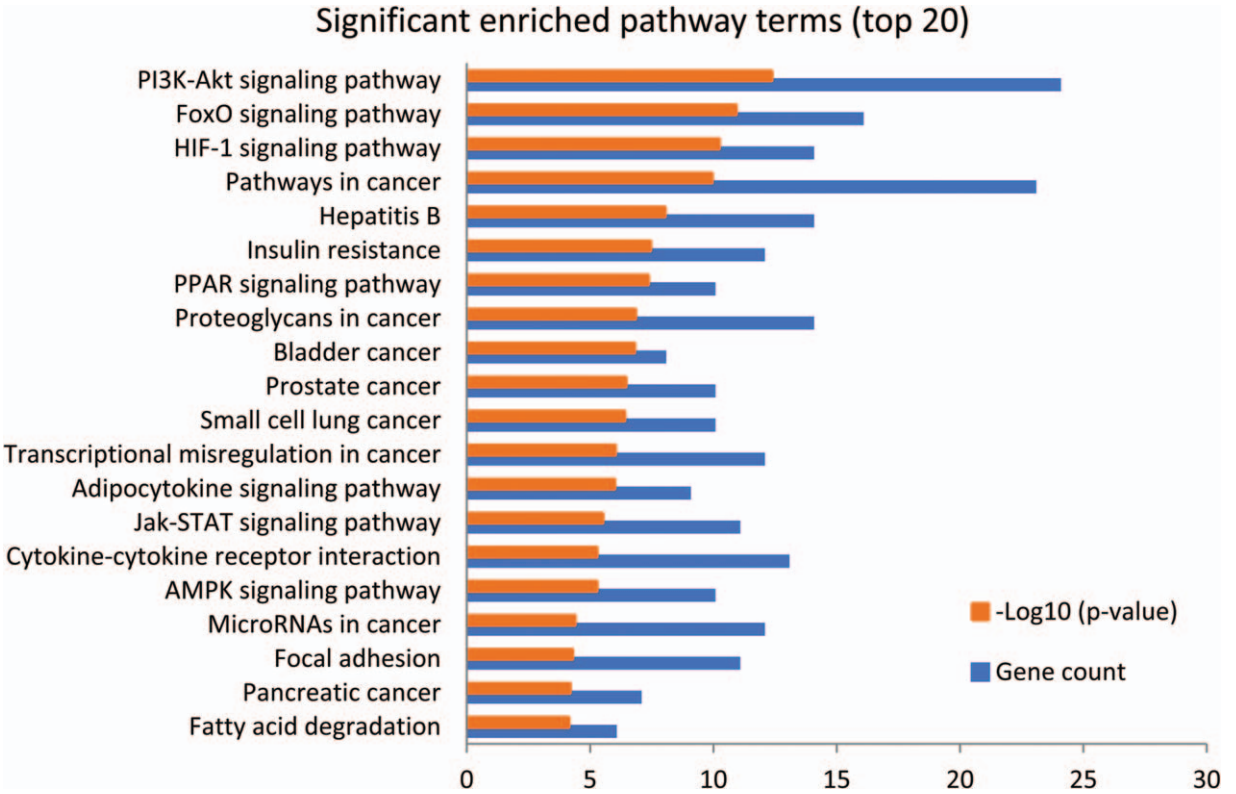

Figure 7. Significantly enriched pathway terms of target genes in the miRNA–TF–gene networks. HIF = hypoxia-inducible factor, miRNA = microRNA, PPAR = peroxisome proliferator-activated receptor, TF = transcription factor.

suppresses multiple myeloma progression by modulating the PTEN/PI3K/Akt signaling pathway.

TFs are the final players of signal transduction cascades, which often begin with extracellular ligand-binding events, followed by signal integration and processing, ultimately resulting in the initiation or repression of target gene transcription.[35] MiRNAs and TFs combine together in a functional network to alter gene expression in cancer.[36]

In CRC, Wang et al[37] generated a miRNA–TF regulatory network, in which 2 miRNAs (hsa-mir-25 and hsa-mir-31), 1 TF breast cancer susceptibility protein (BRCA1), and 2 genes (ADAMTSL3 and AXIN1) were identified as the hub molecules

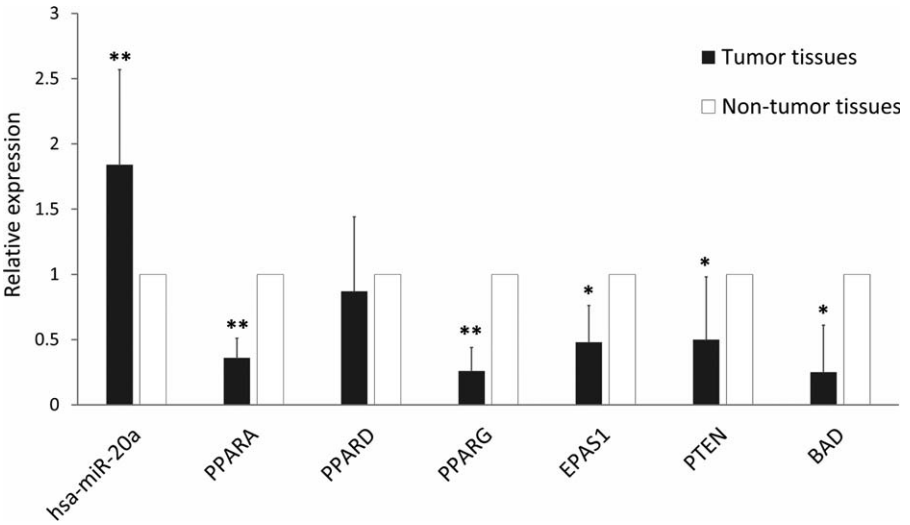

Figure 8. Expression of hsa-miR-20a, TFs, and PI3K-Akt signaling pathway-related genes in CRC tumor tissues and adjacent nontumor tissues. The statistical significance level is indicated by asterisks; * and ** represent *P* values lower than 0.05 and 0.01, respectively. BAD = B-cell lymphoma 2-associated agonist of cell death, PPAR = peroxisome proliferator-activated receptor, PTEN = phosphatase and tensin homolog deleted on chromosome 10.

and as having crucial roles in CRC pathogenesis. MiRNA and TF regulatory networks are activated by the effect of the TFs on the target gene and post-transcription interactions between miRNAs and the target genes separately.[38] In the present study, by predicting the targets of the DEMs and associated cancer-related TFs, we constructed miRNA–TF–gene networks related to the modes of transcription regulation in CRC. From the networks, we found that the most important TFs are peroxisome proliferator-activated receptors (PPARs), which are the predicted targets of miR-20a and interact with the largest number of target genes in the networks. PPARs are ligand-activated TFs that belong to the nuclear-hormone receptor superfamily.[39] There are 3 distinct members of the PPAR family: PPARA, PPARB/D, and PPARG.[40] All 3 members of the PPAR subfamily of nuclear receptors have been shown to participate in energy metabolism: PPARA and PPARB/D function mostly as catabolic regulators of energy expenditure, while PPARG regulates anabolic metabolism, playing a role in energy storage.[41] Besides energy metabolism, PPAR subfamily members also regulate many biological processes, including cell proliferation, survival, apoptosis, and tumor growth.[42] Gao et al[43] reported that PPARA functions as an E3 ubiquitin ligase to induce Bcl2 ubiquitination and degradation, inducing colon cancer cell apoptosis. PPARG is considered to have anticarcinogenic effects in many different cancers, because of its antiproliferation, prodifferentiation, and proapoptotic properties.[44] Shimada et al[45] reported that the PPARG ligand induces apoptosis in colon cancer cells by compensating for deregulated c-Myc expression caused by mutated adenomatous polyposis coli. Whether PPARD ligands potentiate or suppress colon carcinogenesis is debated. For example, in the above study by Shimada et al,[45] no apoptotic effect of PPARD was found in colon cancer cells. Meanwhile, Zhang et al[46] indicated that PPARD directly regulated the transcription of neutral amino acid transporter solute carrier family 1 member 5 and glucose transporter-1 genes, leading to the uptake of glucose and amino acid, activation of mammalian target of rapamycin signaling, and tumor progression in colon cancer cells. However, a study by Yang et al[47] demonstrated that *PPARD* knockdown promotes the growth of colon cancer by inducing less differentiation and accelerating vascular endothelial growth factor (VEGF) expression in tumor cells in vivo; in other words, the study indicated that PPARD attenuates colon carcinogenesis. In the present study, the expression levels of PPARA and PPARG were lower in CRC tumor tissues compared with adjacent nontumor tissues, as confirmed by qRT-PCR, but there was no difference in PPARD expression, suggesting that PPARA and PPARG might have an antitumor role in CRC. However, whether they are direct targets of miRNA-20a and how warrant further experimental verification.

The PI3K/Akt pathway is an important intracellular signal transduction pathway to control the progression of tumor cells, including apoptosis, transcription, translation, metabolism, and angiogenesis.[48] During malignant transformation, various genetic alterations may occur in any of the PI3K pathway components, such as the receptor tyrosine kinase genes EGFR, HER2, KIT, PTEN, PIK3CA, and AKT.[49] By KEGG analysis in the present study, we found that the PI3K/Akt signaling pathway was the most significantly enriched pathway in the miRNA–TF–gene networks. Simultaneously, we found 2 important genes in the miRNA–TF–gene networks: PTEN and BAD. As a negative regulator of PI3K/Akt signaling, PTEN is closely correlated with the carcinogenesis, progression, and prognosis of CRC. A study by Hsu[50] demonstrated that the expression of PTEN in CRC was lower than that in normal colon mucosa, and negative expression of PTEN was correlated with tumor size and poor prognosis in CRC. As an important downstream target of PI3K/Akt signaling, BAD can promote apoptosis by binding B-cell lymphoma 2 and inhibiting its function.[51] In the present study, the expression levels of PTEN and BAD were lower in CRC tumor tissues compared with adjacent nontumor tissues, as confirmed by qRT-PCR, suggesting that PTEN and BAD might play an inhibitory role in CRC. Nevertheless, further research needs to explore the underlying mechanisms in more detail.

In conclusion, using profile datasets of multiple cohorts and integrated bioinformatics analysis, we identified 5 miRNAs that might regulate CRC proliferation through 8 TFs and 116 target genes. On the basis of the results, we constructed miRNA-related TF regulatory networks underlying human CRC. The findings of the potential antitumor roles of PPARA and PPARG and inhibitory roles of PTEN and BAD in CRC have improved the understanding of the molecular basis of CRC. The identified pivotal miRNAs, genes, and pathways could be used as therapeutic targets and diagnostic biomarkers in CRC.

Author contributions

Conceptualization: Guizhen Zhang.
Data curation: Zhenwu Du.
Funding acquisition: Guizhen Zhang.
Investigation: Shuhong Hao, Zhenwu Du.
Methodology: Guizhen Zhang, Shuhong Hao.
Project administration: Guizhen Zhang.
Resources: Sibo Huo, Tongjun Liu.
Software: Shuhong Hao, Ming Ren, Shui Liu.
Visualization: Qiwei Yang.
Writing – original draft: Shuhong Hao.
Writing – review & editing: Shuhong Hao.

References

[1] Siegel R, Desantis C, Jemal A. Colorectal cancer statistics, 2014. CA Cancer J Clin 2014;64:104–17.
[2] Siegel RL, Miller KD, Jemal A. Cancer statistics, 2016. CA Cancer J Clin 2016;66:7–30.
[3] Wang F, Wang J, Cao X, et al. Hsa_circ_0014717 is downregulated in colorectal cancer and inhibits tumor growth by promoting p16 expression. Biomed Pharmacother 2018;98:775–82.
[4] Jia HL, Zeng XQ, Huang F, et al. Integrated microRNA and mRNA sequencing analysis of age-related changes to mouse thymic epithelial cells. IUBMB Life 2018;70:678–90.
[5] Xu P, Zhu Y, Sun B, Xiao Z. Colorectal cancer characterization and therapeutic target prediction based on microRNA expression profile. Sci Rep 2016;6:20616.
[6] Bracken CP, Scott HS, Goodall GJ. A network-biology perspective of microRNA function and dysfunction in cancer. Nat Rev Genet 2016;17:719–32.
[7] Sun M, Song H, Wang S, et al. Integrated analysis identifies microRNA-195 as a suppressor of Hippo-YAP pathway in colorectal cancer. J Hematol Oncol 2017;10:79.
[8] Qu R, Hao S, Jin X, et al. MicroRNA-374b reduces the proliferation and invasion of colon cancer cells by regulation of LRH-1/Wnt signaling. Gene 2018;642:354–61.
[9] Dai Q, Li J, Zhou K, et al. Competing endogenous RNA: a novel post transcriptional regulatory dimension associated with the progression of cancer. Oncol Lett 2015;10:2683–90.
[10] Lambert M, Jambon S, Depauw S, et al. Targeting transcription factors for cancer treatment. Molecules 2018;23:

[11] Wang B, Hsu SH, Wang X, et al. Reciprocal regulation of microRNA-122 and c-Myc in Hepatocellular Cancer: role of E2F1 and transcription factor dimerization partner 2. Hepatology 2014;59:555–66.
[12] Bao M, Song Y, Xia J, et al. miR-1269 promotes cell survival and proliferation by targeting tp53 and caspase-9 in lung cancer. Onco Targets Ther 2018;11:1721–32.
[13] Sullivan KD, Galbraith MD, Andrysik Z, et al. Mechanisms of transcriptional regulation by p53. Cell Death Differ 2018;25:133–43.
[14] Oliveros, J.C. (2007-2015) Venny. An interactive tool for comparing lists with Venn's diagrams. Available at: http://bioinfogp.cnb.csic.es/tools/venny/index.html.
[15] Kozomara A, Griffiths-Jones S. miRBase: annotating high confidence microRNAs using deep sequencing data. Nucleic Acids Res 2014;42:D68–73.
[16] Li JH, Liu S, Zhou H, et al. starBase v2.0: decoding miRNA-ceRNA, miRNA-ncRNA and protein-RNA interaction networks from large-scale CLIP-Seq data. Nucleic Acids Res 2014;42:D92–7.
[17] Zhao F, Xuan Z, Liu L, et al. TRED: a transcriptional regulatory element database and a platform for in silico gene regulation studies. Nucleic Acids Res 2005;1:D103–7.
[18] Han H, Cho JW, Lee S, et al. TRRUST v2: an expanded reference database of human and mouse transcriptional regulatory interactions. Nucleic Acids Res 2018;46(D1):D380–6.
[19] Chandrashekar DS, Bashel B, Balasubramanya SA, et al. UALCAN: a portal for facilitating tumor subgroup gene expression and survival analyses. Neoplasia 2017;19:649–58.
[20] Ashburner M, Ball CA, Blake JA, et al. Gene ontology: tool for the unification of biology. The Gene Ontology Consortium. Nat Genet 2000;25:25–9.
[21] Kanehisa M, Goto S. KEGG: Kyoto encyclopedia of genes and genomes. Nucleic Acids Res 2000;28:27–30.
[22] Huang DW, Sherman BT, Tan Q, et al. The DAVID gene functional classification tool: a novel biological module-centric algorithm to functionally analyze large gene lists. Genome Biol 2007;8:R183.
[23] Livak KJ, Schmittgen TD. Analysis of relative gene expression data using real-time quantitative PCR and the 2 (-Delta Delta C (T)) method. Methods 2001;25:402–8.
[24] Duffy MJ. Use of biomarkers in screening for cancer. Adv Exp Med Biol 2015;867:27–39.
[25] Li B, Ding CM, Li YX, et al. MicroRNA–145 inhibits migration and induces apoptosis in human non–small cell lung cancer cells through regulation of the EGFR/PI3K/AKT signaling pathway. Oncol Rep 2018;40:2944–54.
[26] Xu Y, Chen J, Gao C, et al. MicroRNA-497 inhibits tumor growth through targeting insulin receptor substrate 1 in colorectal cancer. Oncol Lett 2017;14:6379–86.
[27] Jin H, Shi X, Zhao Y, et al. MicroRNA-30a mediates cell migration and invasion by targeting metadherin in colorectal cancer. Technol Cancer Res Treat 2018;17: 1533033818758108.
[28] Zhao G, Han C, Zhang Z, et al. Increased expression of microRNA-31-5p inhibits cell proliferation, migration, and invasion via regulating Sp1 transcription factor in HepG2 hepatocellular carcinoma cell line. Biochem Biophys Res Commun 2017;490:371–7.
[29] Zhao S, Yao D, Chen J, et al. MiR-20a promotes cervical cancer proliferation and metastasis in vitro and in vivo. PLoS One 2015;10: e0120905.
[30] Cheng D, Zhao S, Tang H, et al. MicroRNA-20a-5p promotes colorectal cancer invasion and metastasis by downregulating Smad4. Oncotarget 2016;7:45199–213.
[31] Xu T, Jing C, Shi Y, et al. microRNA-20a enhances the epithelial-to-mesenchymal transition of colorectal cancer cells by modulating matrix metalloproteinases. Exp Ther Med 2015;10:683–8.
[32] Kappel A, Keller A2. MiRNA assays in the clinical laboratory: workflow, detection technologies and automation aspects. Clin Chem Lab Med 2017;55:636–47.
[33] Fan J, Li J, Fan Q. Naringin promotes differentiation of bone marrow stem cells into osteoblasts by upregulating the expression levels of microRNA-20a and downregulating the expression levels of PPARγ. Mol Med Rep 2015;12:4759–65.
[34] Jiang Y, Chang H, Chen G. Effects of microRNA-20a on the proliferation, migration and apoptosis of multiple myeloma via the PTEN/PI3K/AKT signaling pathway. Oncol Lett 2018;15:10001–7.
[35] Wiedemann B, Weisner J, Rauh D. Chemical modulation of transcription factors. Medchemcomm 2018;9:1249–72.
[36] Xin Lai , Wolkenhauer O, Vera J. Understanding microRNA-mediated gene regulatory networks through mathematical modelling. Nucleic Acids Res 2016;44:6019–35.
[37] Wang H, Luo J, Liu C, et al. Investigating MicroRNA and transcription factor co-regulatory networks in colorectal cancer. BMC Bioinformatics 2017;18:388.
[38] Alidadiani N, Ghaderi S, Dilaver N, et al. Epithelial mesenchymal transition Transcription Factor (TF): the structure, function and microRNA feedback loop. Gene 2018;674:115–20.
[39] Bookout AL, Jeong Y, Downes M, et al. Anatomical profiling of nuclear receptor expression reveals a hierarchical transcriptional network. Cell 2006;126:789–99.
[40] Dreyer C, Krey G, Keller H, et al. Control of the peroxisomal beta-oxidation pathway by a novel family of nuclear hormone receptors. Cell 1992;68:879–87.
[41] Pyper SR, Viswakarma N, Yu S, et al. PPARalpha: energy combustion, hypolipidemia, inflammation and cancer. Nucl Recept Signal 2010;8: e002.
[42] Magadum A, Engel FB. PPARβ/δ: linking metabolism to regeneration. Int J Mol Sci 2018;19:E2013.
[43] Gao J, Liu Q, Xu Y, et al. PPARα induces cell apoptosis by destructing Bcl2. Oncotarget 2015;6:44635–42.
[44] Michalik L, Desvergne B, Wahli W. Peroxisome-proliferator-activated receptors and cancers: complex stories. Nat Rev Cancer 2004;4:61–70.
[45] Shimada T, Kojima K, Yoshiura K, et al. Characteristics of the peroxisome proliferator activated receptor gamma (PPARgamma) ligand induced apoptosis in colon cancer cells. Gut 2002;50:658–64.
[46] Zhang W, Xu Y, Xu Q, et al. PPARδ: promotes tumor progression via activation of Glut1 and SLC1-A5 transcription. Carcinogenesis 2017;38:748–55.
[47] Yang L, Zhou J, Ma Q, et al. Knockdown of PPARδ gene promotes the growth of colon cancer and reduces the sensitivity to bevacizumab in nude mice model. PLoS One 2013;8:e60715.
[48] Ke J, Ma P, Chen J, et al. LGR6 promotes the progression of gastric cancer through PI3K/AKT/mTOR pathway. Onco Targets Ther 2018;11:3025–33.
[49] Jang SH, Kim KJ, Oh MH, et al. Clinicopathological significance of elevated PIK3CA expression in gastric cancer. J Gastric Cancer 2016;16:85–92.
[50] Hsu CP, Kao TY, Chang WL, et al. Clinical significance of tumor suppressor PTEN in colorectal carcinoma. Eur J Surg Oncol 2011;37:140–7.
[51] Datta SR, Brunet A, Greenberg ME. Cellular survival: a play in three Akts. Genes Dev 1999;13:2905–27.